

The orbital period of the dipping, bursting, globular cluster X-ray source XB 1746–371 from *Rossi X-ray Timing Explorer* observations

M. Bałucińska-Church,^{1,2*} M. J. Church^{1,2} and A. P. Smale^{3,4}

¹University of Birmingham, School of Physics and Astronomy, Birmingham, B15 2TT

²Astronomical Observatory, Jagiellonian University, ul. Orła 171, 30-244 Cracow, Poland

³Laboratory for High Energy Astrophysics, Code 660.1, NASA/Goddard Space Flight Center, Greenbelt, MD 20771, USA

⁴Office of Space Science, Astronomy and Physics Division, Code SZ, NASA Headquarters, Washington, DC 20546-0001, USA

Accepted 2003 September 15. Received 2003 August 1; in original form 2003 July 7

ABSTRACT

We present results from two long observations of XB 1746–371 by the *Rossi X-ray Timing Explorer* (*RXTE*) in 2002 January and May, lasting 4 and 5 d, respectively. Dips are observed in the X-ray light curves with a depth of 25 per cent, largely independent of energy within the usable band of the PCA instrument of 2.1–16.0 keV. X-ray bursting and flaring activity are also evident. The dips define the orbital period of the system, and using a power spectral analysis and a cycle counting technique, we derive an accurate period of $P_{\text{orb}} = 5.16 \pm 0.01$ h. The previously reported candidate period of 5.73 ± 0.15 h, obtained using *Ginga* data, is inconsistent with our determination, perhaps owing to the weakness of the dipping and the variability of the source during that observation. The dips in the *RXTE* observations presented here do not align with the *Ginga* period; however, our improved period is consistent with a wide range of archival data.

Key words: accretion, accretion discs – binaries: close – stars: individual: XB 1746–371 – stars: neutron – X-rays: binaries.

1 INTRODUCTION

XB 1746–371 is one of the group of ~ 10 low-mass X-ray binaries (LMXBs) exhibiting X-ray dipping at the orbital period, generally accepted as being due to absorption in the bulge in the outer accretion disc. These sources provide substantially more diagnostics and information on the geometry, size and properties of the X-ray emission regions than non-dipping sources. First, there is strong, complex, spectral evolution in dipping; a successful emission model must be able to realistically fit spectra selected in intensity bands through the dips, as well as the non-dip spectrum. In recent years, all of the dipping sources have been fitted by a model consisting of point-like blackbody emission from the surface of the neutron star which causes fast variability in dipping, plus Comptonized emission from an extended accretion disc corona (ADC) (Church et al. 1997, 1998a,b; Bałucińska-Church et al. 1999, 2000; Smale, Church & Bałucińska-Church 2001, 2002). Secondly, the technique of dip ingress timing allows measurement of the size of extended emission regions, when overlapped by an absorber of larger angular size. This reveals that the ADC is very large, of radial extent r_{ADC} typically 50 000 km, and that r_{ADC} increases with source luminosity (Church & Bałucińska-Church 2004) such that in the brightest dipping source

X 1624–490, r_{ADC} becomes 700 000 km, or 65 per cent of the radius of the accretion disc. Thirdly, long-term monitoring of the light curves of the dipping sources may reveal evolution in the orbital period or other effects. This is the case in the source XB 1916–053 having an X-ray period of ~ 3000 s, 1 per cent shorter than the optical period (Chou, Grindlay & Bloser 2001; Homer et al. 2001). In the case of XBT 0748–676, timing studies have been aided by the observation of almost complete X-ray eclipses (Parmar et al. 1986) by the companion star.

XB 1746–371 is a medium-brightness member of the dipping LMXB class in the core of the globular cluster NGC 6441 (Giacconi et al. 1974; Grindlay et al. 1976; Jernigan & Clark 1979; Hertz & Grindlay 1983). Dipping was discovered by Parmar, Stella & Giommi (1989) in an *EXOSAT* observation, indicating a period of 5.0 ± 0.5 h. These dips had a depth of only 15 per cent in the 1–10 keV band, and X-ray bursts were also detected (Sztajno et al. 1987). Sansom et al. (1993) used *Ginga* data to find an orbital period of 5.73 ± 0.15 h. More recently, Jonker et al. (2000) discovered a 1-Hz quasi-periodic oscillation, present during persistent emission and bursts, using *Rossi X-ray Timing Explorer* (*RXTE*) data. An observation with *BeppoSAX* confirmed that dipping was apparently energy-independent, as seen in *EXOSAT* (Parmar et al. 1999), as is also the case in another dipping source X 1755–338 (White et al. 1984; Mason, Parmar & White 1985; Church & Bałucińska-Church 1993). The *BeppoSAX* data implied an orbital period of $5.8^{+0.3}_{-0.9}$ h.

*E-mail: mbc@star.sr.bham.ac.uk

In this paper, we derive an orbital period for XB 1746–371 using *RXTE* observations performed in 2002 January and May, and refine this period using prior *RXTE* observations made in 1996 October and 1998 June–November. We also re-examine archival data from *EXOSAT*, and show that the new period is consistent with all these observations. Our period is inconsistent with the *Ginga* period, and is closer to the original determination by Parmar et al. (1989). In a further paper, we will present results for spectral evolution during dipping and flaring.

2 OBSERVATIONS AND ANALYSIS

We observed XB 1746–371 with *RXTE* (Bradt, Rothschild & Swank 1993) from 2002 January 16 UT 22:42:35 to January 20 UT 21:45:15 (observation ID 60044-02-01-00) and from May 3 UT 14:22:08 to May 8 UT 16:15:15 (observation ID 60044-02-02-00). The observations span nearly 4 and 5 d, respectively. Results presented here use data from the Proportional Counter Array (PCA) operating in Standard 2 mode with 16-s time resolution. The PCA consists of five Xe proportional counter units (PCUs), numbered 0–4, with a combined effective area of about 6500 cm² (Jahoda et al. 1996). PCUs 0 and 2 were reliably on during most of the observations, and we use these PCUs in the following. The propane layer of PCU0 had failed at the start of epoch 5 (defined as 2000, May 13); however, this does not appreciably affect the light curves presented here. Light curves and spectra were extracted using the standard *RXTE* analysis software *FTOOLS* 5.2. Standard screening was applied to select only data with an offset of the telescope pointing axis from the source of $<0.02^\circ$ and an elevation above the Earth’s limb of $>10^\circ$. The source was bright during both observations, with count rates exceeding 40 count s⁻¹ per PCU, and thus the background was calculated using the program *PCABACKEST* with the latest version of the ‘bright’ background model for epoch 5 appropriate to the observations released in 2002 January. The energy band used, 2.1–16.0 keV, was selected by comparison of the spectra of the source + background and the background. At 16 keV, the background was two times smaller than the source + background, and data were not used at energies greater than

this, where the spectra were converging because of the increase of background with energy.

3 RESULTS

The background-subtracted light curves of the 2002 January and May observations are shown in Fig. 1. Both observations reveal dipping with an intensity reduction of 25 per cent. A total of four X-ray bursts can be seen, one of which is double. The peak height of the bursts is reduced substantially by the binning, which is comparable with the total burst duration. In addition, there are periods of X-ray flaring in which the intensity increases by 30 per cent for several thousand seconds. Inspection of light curves in various subbands confirmed that dipping was evident in all energy bands, whereas flaring was only visible above ~ 5 keV. Flaring is well-known in the bright Z-track LMXB sources that are approaching the Eddington limit. However, the luminous dipping source X 1624–490 also exhibits strong flaring dominating the light curve above 8 keV, and the spectral evolution suggests marked changes on the neutron star and at the inner disc (Bałucińska-Church et al. 2001). We have also detected similar flaring in the dipping source XB 1254–490 (Smale et al. 2002). In general, X-ray bursting is observed in faint sources and X-ray flaring is observed in bright sources, so observation of both in the present observation is unusual and presumably reflects the intermediate luminosity of the source. Spectral fitting a non-dip, non-burst, non-flare spectrum gave a 1–30 keV luminosity of 1.36×10^{37} erg s⁻¹ for a distance of 9.0 kpc (Christian & Swank 1997). This is indeed intermediate when compared with X 1624–490 (above), with a non-flaring luminosity of 7×10^{37} – 1.2×10^{38} erg s⁻¹ in *BeppoSAX* and *RXTE* observations (Bałucińska-Church et al. 2000, 2001; for a distance of 15 kpc, Christian & Swank 1997), and with typical burst sources such as XB 1323–619 (Barnard et al. 2001), with luminosities of a few 10^{36} erg s⁻¹.

The orbital period in XB 1746–371 was obtained by a two-stage process. In the first stage, we obtained the power spectrum of the light curve for each observation in the 2.1–3.7 keV band. In this

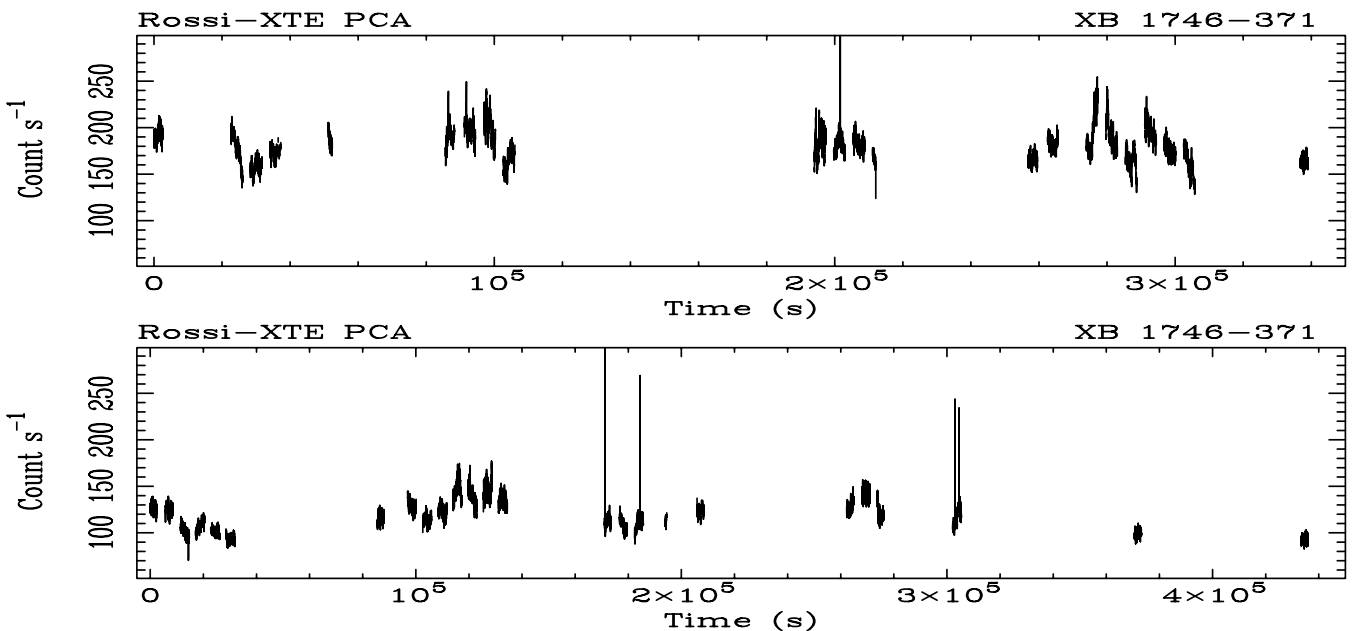


Figure 1. Background-subtracted, PCA light curves of the two observations in PCU0 and PCU2 with 6-s binning in the total usable energy band 2.1–16.0 keV. Upper panel: 2002 January 16–20; lower panel: 2002 May 3–8.

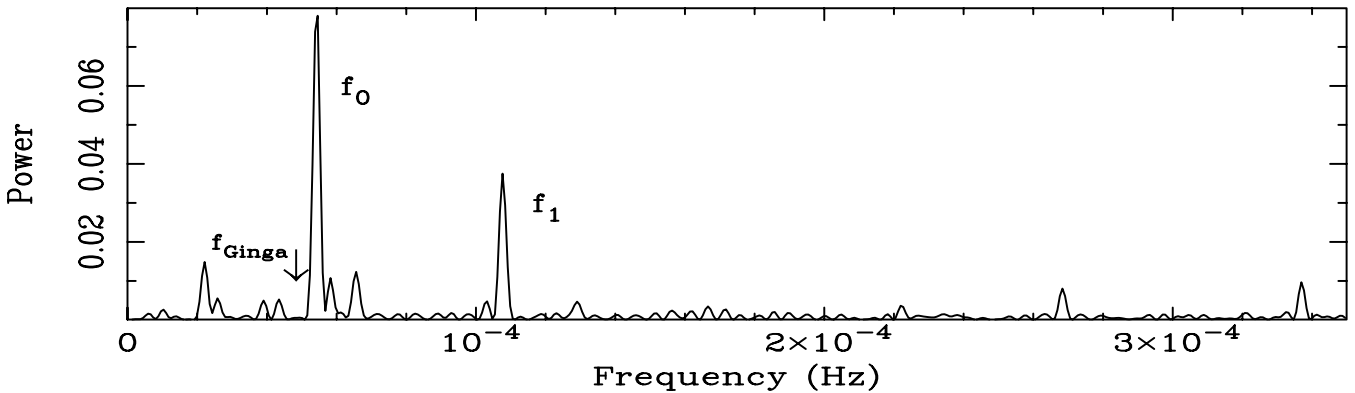


Figure 2. Power spectrum of the 2.1–3.7 keV light curve of the first observation, after removal of the X-ray bursts, removal of the data gaps and detrending.

band, dipping was as strong as in any other band, but flaring was absent, so that spurious peaks in the power spectrum were avoided. The X-ray bursts were also removed from the data to prevent these contaminating the power spectrum. Next, a technique was used to prevent spurious peaks in the power spectrum due to the data gaps caused by Earth occultation and South Atlantic Anomaly (SAA) passage. A modified light curve was made in which real data were given an intensity of unity, and zeroes were written into the data gaps. From this, a window function of the data gaps was obtained which allowed the cleaned spectrum to be obtained by deconvolution of the uncleaned power spectrum and the window function (Roberts, Lehár & Dreher 1987). This was done using the CLEAN algorithm of the PERIOD program, which is part of the STARLINK packages. The incomplete coverage of individual dips did not justify modelling the dip shape to establish the dip centre more accurately. The data were also detrended, although this had little effect on the results.

In principle, a period determination might be made by fitting both observations simultaneously. However, it can be seen from Fig. 1 that the January observation constrains the orbital period well, as there are two clear dips towards the start of the observation and a clear dip close to the end, whereas the second observation only has clear dipping at the start, and these data do not constrain the orbital period well. We therefore obtain the orbital period from the first observation, and then confirm that this period predicts dipping at times observed in the second observation (below). The power spectrum of the first observation is presented in Fig. 2. A strong peak is observed at a frequency (f_0 in Fig. 2) of $5.422 \times 10^{-5} \text{ s}^{-1}$, corresponding to a period of 5.12 h. The uncertainty in this value was obtained by the method of Schwarzenberg-Czerny (1991) using the power spectrum linewidth. This is done by measuring the power of the noise in the neighbourhood of the main peak and obtaining the half-width of the line at a depth of the noise power below the peak which is the 1σ uncertainty. In this case, this gave a half-width in frequency of $\sim 1 \times 10^{-7} \text{ Hz}$. However, this is smaller than the frequency binning in Fig. 2 (optimized in the power spectrum program), which has a half-width of $3.7 \times 10^{-7} \text{ Hz}$, and so we use this to give the uncertainty in the period of $5.12 \pm 0.035 \text{ h}$. There is also a peak (f_1) at a frequency twice f_0 , suggesting that interdipping takes place between the main dips, so that two dips occur in each orbital cycle. The remaining peaks are all small, and most of them are consistent with beating between f_0 or f_1 and the frequencies of Earth occultation and SAA passage, which are related to the 90-min orbital period of the satellite. The period obtained from *Ginga* is indicated by an arrow in Fig. 2, showing that there is no power at this frequency.

Our period determination was then refined by cycle counting techniques using two prior observations of XB 1746–371. Light curves were produced for these observations in the same way as for the data presented above. The first of these, made in 1996 October, was a long observation lasting 600 ks during which clear dipping was observed near the start of the observation at $t = 4000 \text{ s}$ and near the end at $t = 579\,840 \text{ s}$. Using the 5.12-h period, we can deduce that 31 cycles elapsed between these dipping episodes; based on this cycle count, we obtain a period of 5.16 h. It can be seen that the uncertainty of $\pm 0.035 \text{ h}$ accumulates over 31 cycles to 1.09 h, which is 21 per cent of the cycle. Thus, it is unlikely that an error has been made in the cycle count.

A second observation made in 1998 consisted of four subobservations spaced over 6 months. In each of the second and third subobservations, there was one very well defined dip with a deep sharp minimum (other observed dips were not well defined). The time separation of these dips was $8\,317\,920 \text{ s}$, which for a period of 5.16 h gives a cycle count of 447.8. The uncertainty in locating dipping due to the time binning of 16 s gives a negligible error in the period. However, from the three observations used to refine the period, we estimate a period error of $\sim 0.01 \text{ h}$. Using the implied span of periods between 5.15 and 5.17 h gives counts of 448.6 and 446.9, respectively, i.e. the count is 448 ± 1 . Conversely, counts of 449 and 447 correspond to periods of 5.15 and 5.17 h. Thus we cannot be certain that there is not an error of 1 in the count and so obtain from the above timespan and count a period of $5.15(7) \pm 0.01 \text{ h}$.

Finally, we repeated this procedure using the two observations performed in 2002. The time separation between the lowest intensity point in the last dip in the January observation and the lowest point in the first dip in the May observation was $8\,923\,424 \text{ s}$. Using a period of 5.16 h, this gives a cycle count of 480.37 for this separation. For a cycle count of 480, we obtain a period of 5.16(4) h. Thus, we derive a consistent value of the period using 3 observations of $5.16 \pm 0.01 \text{ h}$.

This value of the period was then tested against several light curves as follows. In Fig. 3, we show the present observations and compare the actual dipping with the predicted dip centres based on a period of 5.16 h (lower arrows). We also show the dip centres expected from the *Ginga* period of 5.73 h (upper arrows). For both periods, the first arrow is aligned with the first dip in each observation. It is clear that the 5.16-h period gives very good alignment with the dips observed. In the second observation (2002 May), there is a possible dip at $3.0 \times 10^5 \text{ s}$ which is not well aligned with an arrow. However, the previous dip is at $2.7 \times 10^5 \text{ s}$, which is 7.77 h from the possible dip. Thus it is likely that this is not a real dip

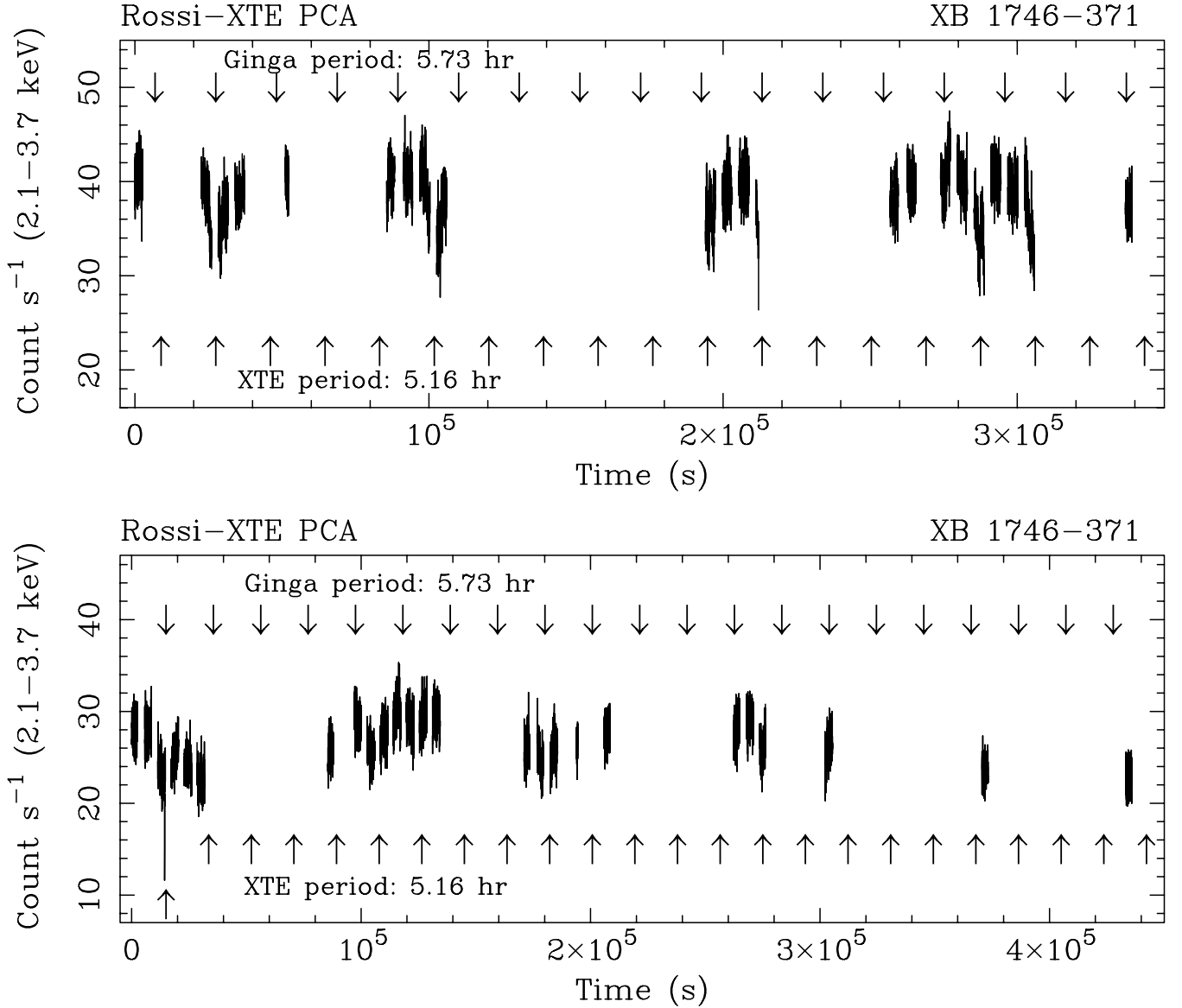


Figure 3. Comparison of the present *RXTE* period and the *Ginga* period with dipping occurrence. Upper panel: 2002 January observation; lower panel: 2002 May observation.

but part of a trend of general intensity decrease that can be seen in the latter part of the observation. The 5.16-h period was also tested against the light curve of the *EXOSAT* observation of 1985 September 9 and gave good alignment. Finally, the two additional *RXTE* observations of 1996 and 1998 used above to refine the period were tested, and good alignment of dipping with the period was obtained.

In Fig. 4, we present the data from the 2002 January *RXTE* observation folded on the best-fit period, together with the corresponding folded hardness ratio, where the hardness is defined as the ratio of the count rates in the 9.8–16.0 and 2.1–3.7 keV bands. The dipping is seen clearly in the folded light curve, with some indication of interdipping between the main dips. The folded hardness ratio confirms that dipping is largely energy independent, as was previously known from the *EXOSAT* and *BeppoSAX* observations (Parmar et al. 1989, 1999). Because flaring may persist during dipping, we cannot say whether the small change in hardness in the dip is due to dipping or to flaring.

4 DISCUSSION

The long observations that we made with *RXTE* have allowed us to derive an improved orbital period of 5.16 ± 0.01 h for XB 1746–371. Comparison with previous orbital period determinations shows that the *EXOSAT* value of 5.0 ± 0.5 h (Parmar et al. 1989) is consistent with our present result, as is the *BeppoSAX* period of $5.8^{+0.3}_{-0.9}$ h (Parmar et al. 1999), but the *Ginga* value of 5.73 ± 0.15 h (Sansom et al. 1993) is not. This is also apparent from Fig. 2, where the *Ginga* value corresponding to a frequency of $4.84 \times 10^{-5} \text{ s}^{-1}$ lies well to the side of the strongest peak. Inspection of Figs 3 and 4 also shows that the *Ginga* period is inconsistent with the present data. In the 2002 January observation, the *Ginga* period fails to align with the dipping at $\sim 10^5$ s, or at $\sim 3 \times 10^5$ s, although the arrows are coincidentally aligned with dipping in between these times (at $\sim 2 \times 10^5$ s). We note that dipping in the *Ginga* data was much

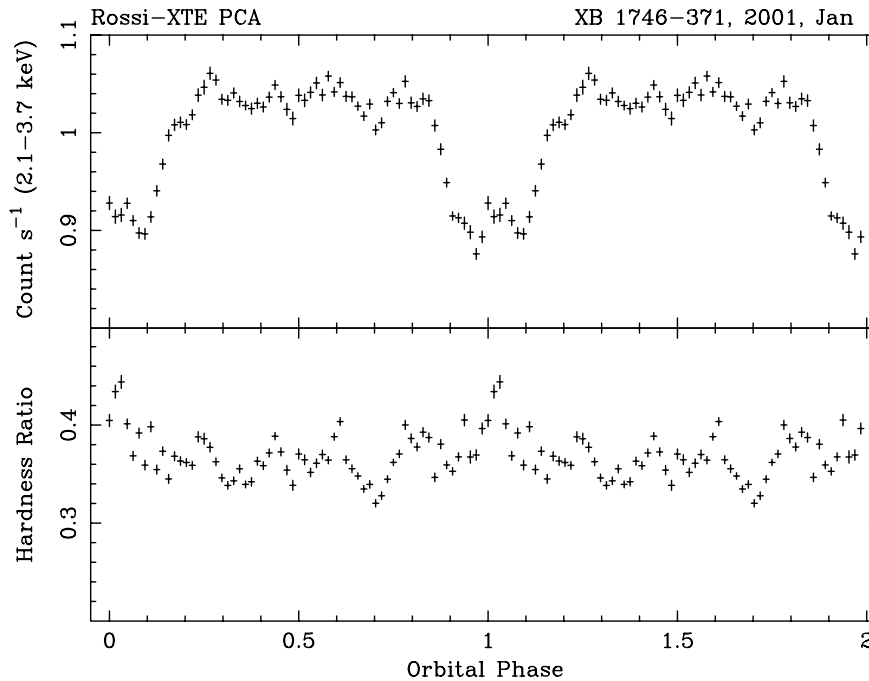


Figure 4. Light curve folded on the orbital period of 5.16 h obtained in the present work for the band 2.1–3.7 keV (see text), together with the hardness ratio (9.8–16.0 keV)/(2.1–3.7 keV). The count rate is normalized by dividing by the mean.

less pronounced than in the present observations, making the period more difficult to determine.

XB 1746–371 is unusual in displaying energy-independent dipping, as does one other dipping source, X 1755–338 (White et al. 1984; Mason et al. 1985; Church & Bałucińska-Church 1993). In the case of the *EXOSAT* observation of XB 1746–371, Parmar et al. (1989) examined possible causes of energy independence, including an ionized absorber. The *BeppoSAX* observation again revealed energy independence in dipping, and Parmar et al. (1999) ruled out possible causes such as an ionized absorber, very low metallicity (reduced by 130 times from Solar) and also the explanation for X 1755–338 of Church & Bałucińska-Church (1993), in which two spectral components combine to give approximate energy independence. We will investigate the spectral evolution during the dips in the present *RXTE* data in a further paper.

ACKNOWLEDGMENTS

This research has made use of data obtained from the High Energy Astrophysics Science Archive Research Centre (HEASARC), provided by NASA’s Goddard Space Flight Centre. The work was supported in part by the Polish KBN grants PBZ-KBN-054/P03/2001 and KBN-2-P03D-015-25.

REFERENCES

- Bałucińska-Church M., Church M. J., Oosterbroek T., Segreto A., Morley R., Parmar A. N., 1999, *A&A*, 349, 495
- Bałucińska-Church M., Humphrey P. J., Church M. J., Parmar A. N., 2000, *A&A*, 360, 583
- Bałucińska-Church M., Barnard R., Church M. J., Smale A. P., 2001, *A&A*, 378, 847
- Barnard R., Bałucińska-Church M., Smale A. P., Church M. J., 2001, *A&A*, 380, 494
- Bradt H. V., Rothschild R. E., Swank J. H., 1993, *A&A*, 97, 335
- Chou Y., Grindlay J. E., Bloser P. F., 2001, *ApJ*, 549, 1135
- Christian D. J., Swank J. H., 1997, *ApJS*, 109, 177
- Church M. J., Bałucińska-Church M., 1993, *MNRAS*, 260, 59
- Church M. J., Bałucińska-Church M., 2004, *MNRAS*, in press
- Church M. J., Mitsuda K., Dotani T., Bałucińska-Church M., Inoue H., Yoshida K., 1997, *ApJ*, 491, 388
- Church M. J., Bałucińska-Church M., Dotani T., Asai K., 1998a, *ApJ*, 504, 516
- Church M. J., Parmar A. N., Bałucińska-Church M., Oosterbroek T., Dal Fiume D., Orlandini M., 1998b, *A&A*, 338, 556
- Giacconi R. et al., 1974, *ApJS*, 27, 37
- Grindlay J. E., Schnopper H., Schreier E., Gursky H., Parsignault D. R., 1976, *ApJ*, 206, L23
- Hertz P., Grindlay J. E., 1983, *ApJ*, 275, 105
- Homer L., Charles P. A., Hakala P., Muhli P., Shih I.-C., Smale A. P., Ramsay G., 2001, *MNRAS*, 322, 827
- Jahoda K., Swank J. H., Giles A. B., Stark M. J., Strohmayer T., Zhang W., Morgan E. H., 1996, *Proc. SPIE*, 2808, 59
- Jernigan J. G., Clark G. W., 1979, *ApJ*, 231, L125
- Jonker P. G. et al., 2000, *ApJ*, 531, 453
- Mason K. O., Parmar A. N., White N. E., 1985, *MNRAS*, 216, 1033
- Parmar A. N., White N. E., Giommi P., Gottwald M., 1986, *ApJ*, 308, 199
- Parmar A. N., Stella L., Giommi P., 1989, *A&A*, 222, 96
- Parmar A. N., Oosterbroek T., Guainazzi M., Segreto A., Dal Fiume D., Stella L., 1999, *A&A*, 351, 225
- Roberts D. H., Lehár J., Dreher J. W., 1987, *AJ*, 93, 968
- Sansom A. E., Dotani T., Asai K., Lehto J. H., 1993, *MNRAS*, 262, 429
- Schwarzenberg-Czerny A., 1991, *MNRAS*, 253, 198
- Smale A. P., Church M. J., Bałucińska-Church M., 2001, *ApJ*, 550, 962
- Smale A. P., Church M. J., Bałucińska-Church M., 2002, *ApJ*, 581, 1286
- Sztajno M., Fujimoto M. Y., van Paradijs J., Vacca W. D., Lewin W. H. G., Penninx W., Trümper J., 1987, *MNRAS*, 226, 39
- White N. E., Parmar A. N., Sztajno M., Zimmermann H. U., Mason K. O., Kahn S., 1984, *ApJ*, 283, L9

This paper has been typeset from a $\text{\TeX}/\text{\LaTeX}$ file prepared by the author.